Journal of Sound and Vibration (1999) **223**(4), 497–512
Article No. jsvi.1998.2120, available online at http://www.idealibrary.com on IDEAL®

VIBRATION CHARACTERISTICS OF A CRACKED ROTOR WITH TWO OPEN CRACKS

A. S. SEKHAR

Department of Mechanical Engineering, Indian Institute of Technology, Kharagpur 721 302, *India*

(*Received* 28 *April* 1998, *and in final form* 20 *October* 1998)

The dynamic behaviour of structures, in particular, that of a rotor, containing cracks is a subject of considerable current interest. Several researchers have developed models of cracked rotor systems considering mainly a single transverse surface crack. In the present study Finite Element (FEM) analysis of a rotor system for flexural vibrations has been considered by including two transverse open cracks The eigenvalue analysis and stability study of a rotor system including a shaft with two open cracks have been carried out and the influence of one crack over the other for eigenfrequencies, mode shapes and for threshold speed limits has been observed.

1. INTRODUCTION

One form of damage that can lead to catastrophic failure if undetected is fatigue cracks in the shaft. Several researchers have developed models of cracked rotor systems in order to predict the change in vibrational behaviour due to crack growth. Many researchers have realized the importance of the cracked structures, in particular the dynamics of cracked rotors, which is well documented in a book by Dimarogonas and Paipetis [1], followed by a literature survey by Wauer [2]; more recently, a survey on simple rotors by Gasch [3] and a review on general cracked structures by Dimarogonas [4] have been published.

However, all the work reported above considers mainly a single transverse crack of the shaft. if the structure is cracked in at least two positions, the problem of crack sizing and location becomes decidedly more complex. The double crack assessment for structures has been addressed by relatively few authors [5–8]. A review on this aspect was done by Ruotolo and Surace [9].

Ostachowicz and Krawczuk [5] have considered a continuous model of a beam with cracks which are modelled by massless rotational springs and evaluated the dynamic behaviour with two cracks, while Shen and Pierre [6] considered symmetric cracks. Surace *et al*. [7, 8] analysed this problem using both continuous models and FEM, together with experimental results with two cracks and studied changes in eigenfrequencies with crack parameters such as location

0022–460X/99/240497 + 16 $30.00/0

and depth. All these studies [5–8] mainly focus on double cracks and on finding the changes in dynamic behaviour when the damage is known.

Development of a generalized state of damage identification procedure for multiple cracks is also of considerable interest currently. The typical approaches are based on optimization [10] and with genetic algorithms [11] as pointed out in reference [9].

The instability of the first and second kind were given by Papadopoulos and Dimarogonas [12] and the method for the determination of intervals for these kinds were developed by the same authors [13]. In the stability chart several sub harmonics of longitudinal and lateral natural frequencies were noticed as thresholds of instability. Thus, it was shown that a surface crack on a rotating shaft can yield a variety of unstable areas of operation due to the coupling of lateral and longitudinal vibration.

Gasch [3] using Floquet theory presented instability zones for a cracked simple rotor with hinge model. Huang *et al.* [14] and Chue *et al.* [15] also examined rotors using the Floquet theory and found that instability occurs as rotation is close to an integer fraction or an integer multiple of shaft bending frequency when the crack depth reaches half the radius.

Ishida *et al.* [16] found that in the case of a comparatively large imbalance, the shape of resonance curves changes markedly depending on the relative angular position of the imbalance to the crack, and an unstable region appears for a certain range of angular positions. Parametric vibrations [17, 18] and chaotic motion [19] were also observed in cracked rotors.

In the present study considering the importance of dynamic behaviour of rotors with double cracks, a parametric study of two transverse open cracks in a rotor has been carried out, for various crack parameters such as crack depth and crack location. It also determines the changes in eigenfrequencies and stability speeds with crack parameters and for shaft parameters such as the slenderness ratio. Most of the earlier studies involved eigenfrequencies on beams, whereas here, the cracks are considered in a rotor and stability limits are also evaluated in the present study.

Finite Element (FEM) analysis of a rotor-bearing system for flexural vibrations has been considered by including two transverse open cracks in the shaft. The eigenvalue analysis and system stability study of the rotor have been carried out to observe the influence of one crack over the other for eigenfrequencies, mode shapes and threshold speed limits. The study has been carried out for two aligned cracks along the axis. However, this can be extended for two cracks in two different directions.

2. SYSTEM EQUATION OF MOTION

Nelson and McVaugh [20] presented a finite element model using Rayleigh beam theory for the rotor–bearing system which consists of rigid discs, distributed parameter finite shaft elements and discrete bearings. Ozguven and Ozkan [21] presented an extended model by synthesizing the previous models.

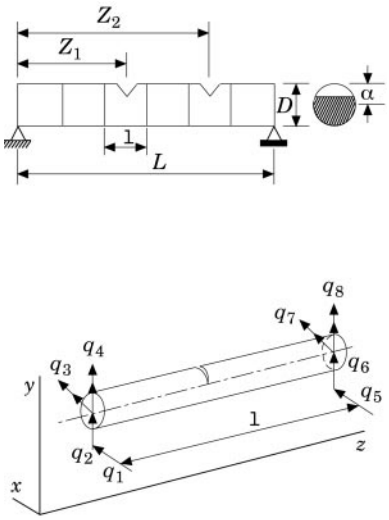

Figure 1. Model rotor system with a cracked element.

The present study uses these models by including the crack model to study the vibration characteristics of the rotor.

The rotor shaft (see Figure 1) is discretized into finite beam elements. As shown in Figure 1, each element has two translational and two rotational degrees of freedom for bending mode at each node represented by $q_1 - q_8$ (though the element is shown with a transverse crack, the degrees of freedom considered are the same for an uncracked element as well). The discrete bearing stiffness and damping and the rigid disc mass parameters are considered at the corresponding degrees of freedom, after assembling the different shaft elements.

The equation of motion of the complete rotor system (see Figure 1) in a fixed co-ordinate system can be written as

$$[\mathbf{M}]\ddot{q} + [\mathbf{D}]\dot{q} + [\mathbf{K}]q = Q \tag{1}$$

where the mass matrix includes the rotary and translational mass matrices of the shaft, rigid disc mass and diametral moments of inertia. The matrix **D** includes the gyroscopic moments and bearing damping. The stiffness matrix considers the stiffnesses of shaft, bearing and of the cracked shaft element. The details of the individual matrices of equation (1) except that of the cracked shaft element are given in reference [20].

The details of the stiffness matrix of the cracked shaft element are discussed in section 3. The eigenvalue analysis has been carried out for a non-gyro, undamped and stationary rotor. The crack has been treated as open. This element will replace the corresponding uncracked element while assembling different rotor components.

3. CRACK MODELLING

In the present study the transverse crack has been considered as open. The flexibility matrix of a cracked section as given in Papadopoulos and Dimarogonas [12] and utilized in the FEM analysis of Sekhar and Prabhu [22] has been used for the crack modelling and the details are presented here.

With the shearing action neglected, and by using the strain energy, the flexibility coefficients for a section of an element without a crack can be derived in the form,

$$\mathbf{C}_0 = \begin{bmatrix} l^3/3EI & & \text{SYM} & \\ 0 & l^3/3EI & & \\ 0 & -l^2/2EI & l/EI & \\ l^2/2EI & 0 & 0 & l/EI \end{bmatrix},$$

which is nothing but the inverse of the stiffness matrix of a section of an uncracked element as obtained in the equation (1). Here l is the length of the element.

A crack on a beam element introduces considerable local flexibility due to strain energy concentration in the vicinity of the crack tip under load. According to the principle of Saint-Venant, the stress field is affected only in the region adjacent to the crack. The element stiffness matrix, except for the cracked element, may be regarded as unchanged under a certain limitation of element size [23]. It is very difficult to find out an appropriate shape function to express the kinetic energy and elastic potential energy approximately, because of the discontinuity of deformation in the cracked element. However, the additional stress energy of a crack has been studied thoroughly in fracture mechanics and the flexibility coefficient, expressed by a stress intensity factor, can be easily derived by means of Castigliano's theorem in the linear elastic range. The shaft can be divided into elements. The behaviour of the elements situated to the right of the cracked element may be regarded as external forces applied to the cracked element, while the behaviour of elements situated to its left may be regarded as constraints [23]. Thus the flexibility matrix of a cracked element with constraints may be calculated. The additional strain energy due to the crack results in a local flexibility matrix

$$\mathbf{C}_c = \frac{1}{F_0} \begin{bmatrix} \bar{c}_{11}R & & \text{SYM} & \\ 0 & \bar{c}_{22}R & & \\ 0 & 0 & \bar{c}_{33}/R & \\ 0 & 0 & \bar{c}_{43}/R & \bar{c}_{44}/R \end{bmatrix},$$

where $F_0 = \pi ER^2/(1-\nu^2)$, $R = D/2$ and $\nu = 0{\cdot}3$.

The dimensionless compliance coefficients, $\bar{c}_{ij}$ of $\mathbf{C}_c$ are computed from the derivations discussed in [12]. One must add the local flexibility due to the crack to obtain the total flexibility of the cracked element. The total flexibility matrix for the cracked matrix for the cracked section is given as $[\mathbf{C}] = [\mathbf{C}_0] + [\mathbf{C}_c]$.

From the equilibrium condition (see Figure 1)

$$(q_1, q_2, \cdots, q_8)^T = [\mathbf{T}](q_5, \cdots, q_8)^T, \tag{2}$$

where the transformation matrix is

$$\mathbf{T} = \begin{bmatrix} -1 & 0 & 0 & 0 \\ 0 & -1 & 0 & 0 \\ 0 & l & -1 & 0 \\ -l & 0 & 0 & -1 \\ 1 & 0 & 0 & 0 \\ 0 & 1 & 0 & 0 \\ 0 & 0 & 1 & 0 \\ 0 & 0 & 0 & 1 \end{bmatrix}.$$

Using the principle of virtual work, the stiffness matrix of the cracked element can be written as [22, 23],

$$[\mathbf{K}_c] = [\mathbf{T}][\mathbf{C}]^{-1}[\mathbf{T}]^T \tag{3}$$

4. EIGENVALUE AND STABILITY ANALYSES

The crack is assumed to effect only stiffness. The stiffness matrix of a cracked element, $\mathbf{K}_c$ will replace the stiffness matrix of the same element prior to cracking to result in the global stiffness matrix $[\bar{\mathbf{K}}]$. Thus the eigenfrequencies and mode shapes are obtained by solving the eigenvalue problems $[\mathbf{K}] - \omega^2[\mathbf{M}] = 0$, and $[\bar{\mathbf{K}}] - \omega^2[\mathbf{M}] = 0$, for the uncracked and cracked rotor systems, respectively.

The eigenvalue analysis has been carried out for a non-gyro, undamped and stationary rotor. The crack has been treated as open. And hence, the stiffness matrix, $[\mathbf{K}_c]$ of the cracked element as evaluated in section 3 replaces the uncracked shaft element to result in the global stiffness matrix $[\bar{\mathbf{K}}]$ of the equation of motion.

The system instability speeds or threshold speeds by including internal damping effects [24] were also obtained by solving for complex eigenvalues $\lambda_i = \zeta_i + j\omega_i$ of the system without and with two cracks. The complex eigenvalues are solved by EISPACK subroutines. The instability speed has been obtained for the first mode from the logarithmic decrement, $\delta = -2\pi\zeta/\omega$. The $\delta < 0$ indicates the stability threshold.

5. RESULTS AND DISCUSSION

The results are obtained by introducing two cracks at different locations on a simply supported steel shaft and compared with uncracked conditions. The crack parameters, the rotor geometries and undamped eigenfrequencies are expressed in dimensionless forms.

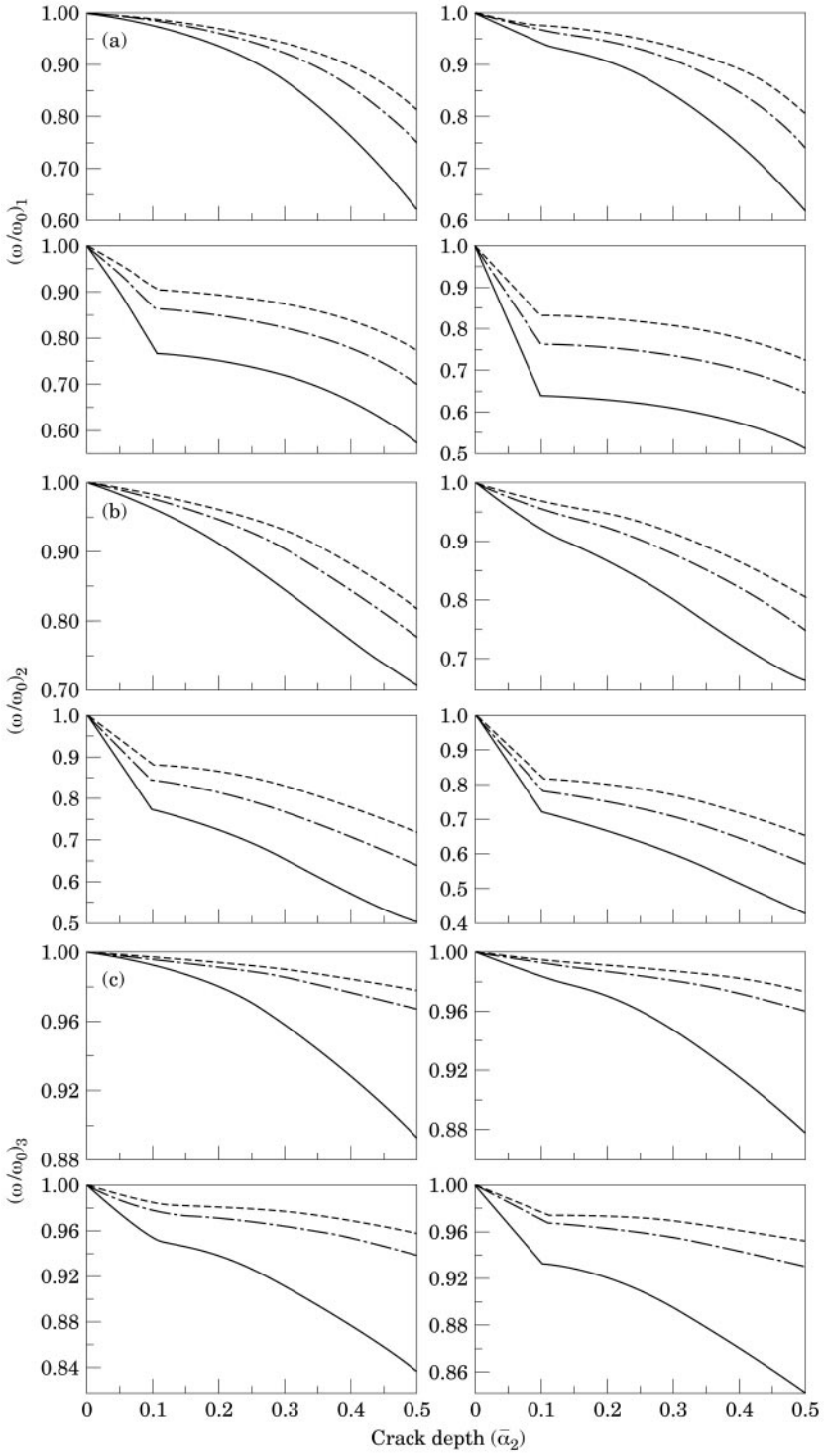

Figure 2. Variation of eigenfrequencies with different crack depths for different shaft geometric ratios. $\bar{\alpha}_1$ for each set: top left 0·1; top right 0·2; bottom left 0·4; bottom right 0·5. Key for L/D values: —, 4·0; –·–, 8·0; - - - -, 12·5 $\times$ — $\times$, with shear effect, $L/D = 4$. (a) first eigenfrequency; (b) second eigenfrequency; (c) third eigenfrequency.

Both forward and backward whirl speeds are present in each mode for the eigenvalue results. However, the forward and minimum eigenfrequency values with an increase in crack are presented.

The first crack is considered at $Z_1/L = 0{\cdot}35$ with crack depth given by $\bar{\alpha}_1 = \alpha_1/D$, while the second crack has $Z_2/L = 0{\cdot}65$, with a crack depth of $\bar{\alpha}_2 = \alpha_2/D$. The rotors with various slenderness ratios, L/D are considered (refer to Figure 1).

The variations of normalized (with respect to rotor with first crack) eigenfrequencies with the depth of the second crack for different modes and different shaft geometric ratios are shown in Figures 2(a–c). The corresponding mode shapes for first and second modes are shown in Figures 3(a, b). It is seen

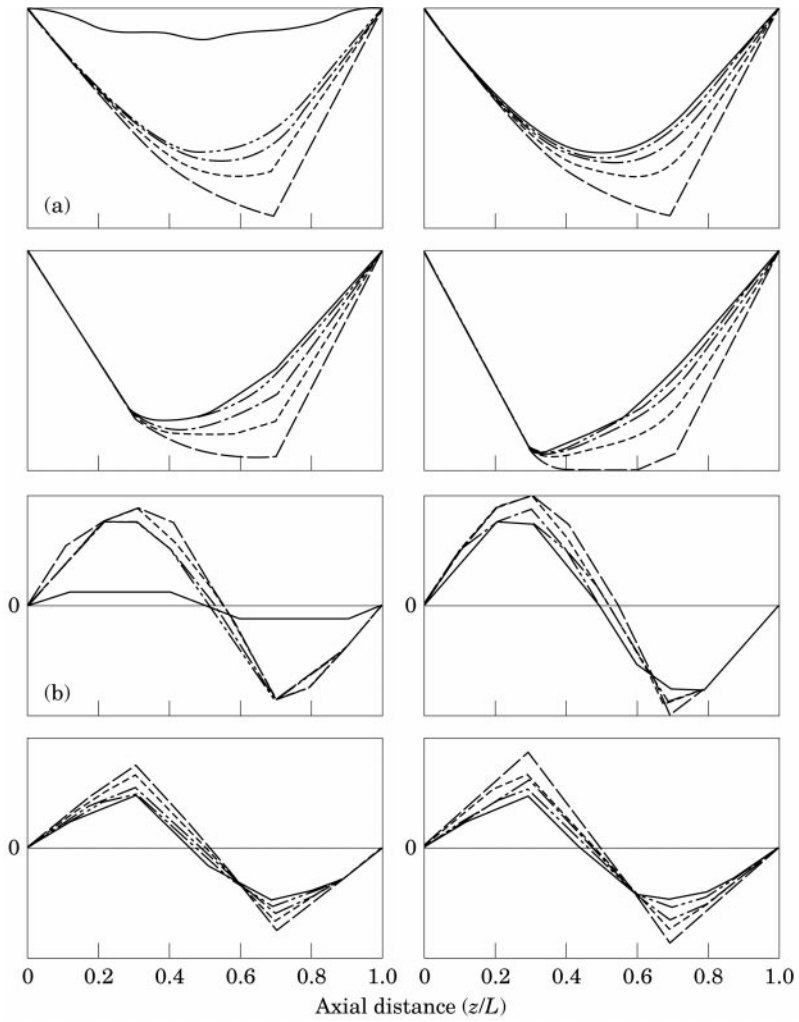

Figure 3. Rotor mode shapes for different crack parameters with $L/D = 4$. $\bar{\alpha}_1$ values as for Figure 2. Key for $\bar{\alpha}_2$ values: —, 0·1; – - - –, 0·2; — - —, 0·3; - - - -, 0·4; – – –, 0·5. (a) first eigenfrequency; (b) second eigenfrequency.

clearly from the Figures 2(a–c) that the changes in eigenfrequencies due to a crack are appreciable in cases of shafts with low slenderness ratio (L/D), similar to that reported in [22] for rotors with a single crack. As the cracks are closer to the antinodal points in the case of the second mode and the second crack is closer to the antinode (center) in the case of first mode, the changes in eigenfrequencies with crack present are quite significant. However, in the case of the third mode the changes are quite low except for deeper cracks, as the cracks are near to the nodal point of that mode. Due to the shift in the node positions for higher modes the changes in eigenfrequency and mode shape depend on how close the crack is to the mode shape node.

The eigenvalue analysis has been carried out by including shear effects [25] also in the case of $L/D = 4$. Here also the normalization is done with the eigenfrequency (with shear effect in this case) of the uncracked rotor. The results are presented in Figures 2(a–c).

The effect of shear influences the eigenfrequencies of the cracked rotor also. But it can be noticed from Figures 2(a–c) that the difference between the variations of normalized eigenfrequencies with crack depth for the cases of with

TABLE 1

Variation of normalized first eigenfrequencies with crack parameters, $L/D = 8$

	Z_2/L				
α_2/D	0·15	0·3	0·5	0·7	0·85
	$Z_1/L = 0{\cdot}35$, $\alpha_1/D = 0{\cdot}1$				
0·1	0·9871	0·9828	0·9801	0·9840	0·9882
0·2	0·9785	0·9626	0·9522	0·9668	0·9840
0·3	0·9604	0·9218	0·8989	0·9320	0·9752
0·4	0·9268	0·8539	0·8159	0·8725	0·9585
0·5	0·8648	0·7488	0·6972	0·7760	0·9250
	$Z_1/L = 0{\cdot}35$, $\alpha_1/D = 0{\cdot}25$				
0·1	0·9409	0·9375	0·9350	0·9384	0·9419
0·2	0·9334	0·9194	0·9106	0·9235	0·9384
0·3	0·9174	0·8833	0·8636	0·8934	0·9308
0·4	0·8878	0·8230	0·7894	0·8413	0·9165
0·5	0·8335	0·7279	0·6810	0·7549	0·8882
	$Z_1/L = 0{\cdot}35$, $\alpha_1/D = 0{\cdot}35$				
0·1	0·8785	0·8757	0·8738	0·8765	0·8793
0·2	0·8723	0·8608	0·8539	0·8647	0·8765
0·3	0·8589	0·8306	0·8148	0·8400	0·8705
0·4	0·8343	0·7795	0·7515	0·7968	0·8589
0·5	0·7886	0·6972	0·6564	0·7232	0·8360
	$Z_1/L = 0{\cdot}35$, $\alpha_1/D = 0{\cdot}45$				
0·1	0·7834	0·7815	0·7799	0·7820	0·7840
0·2	0·7790	0·7709	0·7663	0·7741	0·7815
0·3	0·7694	0·7488	0·7378	0·7568	0·7780
0·4	0·7514	0·7102	0·6898	0·7253	0·7700
0·5	0·7169	0·6458	0·6140	0·6694	0·7537

TABLE 2

Variation of normalized second eigenfrequencies with crack parameters, $L/D = 8$

	Z_2/L				
α_2/D	0·15	0·3	0·5	0·7	0·85
	$Z_1/L = 0{\cdot}35$, $\alpha_1/D = 0{\cdot}1$				
0·1	0·9849	0·9854	0·9934	0·9839	0·9871
0·2	0·9615	0·9638	0·9925	0·9569	0·9724
0·3	0·9162	0·9261	0·9907	0·9097	0·9417
0·4	0·8466	0·8755	0·9879	0·8468	0·8877
0·5	0·7544	0·8182	0·9840	0·7756	0·7999
	$Z_1/L = 0{\cdot}35$, $\alpha_1/D = 0{\cdot}25$				
0·1	0·9626	0·9631	0·9694	0·9597	0·9631
0·2	0·9429	0·9452	0·9679	0·9315	0·9483
0·3	0·9039	0·9133	0·9649	0·8821	0·9176
0·4	0·8413	0·8691	0·9604	0·8163	0·8638
0·5	0·7537	0·8163	0·9543	0·7420	0·7767
	$Z_1/L = 0{\cdot}35$, $\alpha_1/D = 0{\cdot}35$				
0·1	0·9358	0·9363	0·9407	0·9309	0·9348
0·2	0·9203	0·9226	0·9382	0·9014	0·9199
0·3	0·8882	0·8972	0·9334	0·8494	0·8890
0·4	0·8342	0·8604	0·9257	0·7796	0·8351
0·5	0·7528	0·8136	0·9151	0·7003	0·7484
	$Z_1/L = 0{\cdot}35$, $\alpha_1/D = 0{\cdot}45$				
0·1	0·9017	0·9022	0·9044	0·8948	0·8990
0·2	0·8908	0·8932	0·9002	0·8641	0·8844
0·3	0·8671	0·8755	0·8921	0·8088	0·8536
0·4	0·8239	0·8478	0·8785	0·7336	0·7994
0·5	0·7514	0·8094	0·8588	0·6466	0·7125

and without shear effects is not much except in mode III (Figure 2c), where the reduction in normalized eigenfrequency as such is very low. Hence, all other results are calculated for the cases without shear effects.

From the mode shapes shown in Figures 3(a, b) it can be observed very clearly the changes in slopes and deviations are due to cracks in mode shapes at crack positions of $Z/L = 0{\cdot}35$ and 0·65. Thus extending this for various crack locations and depths one can construct a contour diagram of eigenfrequencies for each crack position and depth. According to this diagram, the depth of the crack can be read from its cracked eigenfrequency if the position of crack is known from the sharply changed curves of deviation of the mode shape [26].

It can be seen from Figure 2a that in the presence of the first crack with sufficient depth ($\bar{\alpha}_1 = 0{\cdot}2$), a second crack with even a small depth caused a large drop in eigenfrequency (see Figure 2a with second crack of depth 0·1).

A parametric study by varying the cracks' locations (Z/L) and depths, (α/D) of a rotor of $L/D = 8$, for both eigenvalue analysis and stability limits has been carried out with the results shown in Table 1–6. For this study of both eigenvalue and stability analysis the normalization is done with that of an uncracked rotor.

TABLE 3

Variation of normalized third eigenfrequencies with crack parameters, $L/D = 8$

	Z_2/L				
α_2/D	0·15	0·3	0·5	0·7	0·85
	$Z_1/L = 0{\cdot}35$, $\alpha_1/D = 0{\cdot}1$				
0·1	0·9866	0·9982	0·9889	0·9972	0·9882
0·2	0·9587	0·9969	0·9628	0·9902	0·9635
0·3	0·9137	0·9946	0·9185	0·9785	0·9170
0·4	0·8618	0·9910	0·8623	0·9638	0·8518
0·5	0·8141	0·9863	0·8036	0·9478	0·7806
	$Z_1/L = 0{\cdot}35$, $\alpha_1/D = 0{\cdot}25$				
0·1	0·9741	0·9868	0·9791	0·9859	0·9780
0·2	0·9425	0·9851	0·9558	0·9794	0·9555
0·3	0·8909	0·9819	0·9151	0·9683	0·9123
0·4	0·8316	0·9771	0·8612	0·9544	0·8498
0·5	0·7767	0·9709	0·8022	0·9395	0·7798
	$Z_1/L = 0{\cdot}35$, $\alpha_1/D = 0{\cdot}35$				
0·1	0·9584	0·7227	0·9663	0·9717	0·9650
0·2	0·9225	0·9697	0·9466	0·9656	0·9452
0·3	0·8629	0·9649	0·9104	0·9552	0·9059
0·4	0·7929	0·9577	0·8598	0·9424	0·8470
0·5	0·7295	0·9486	0·8010	0·9287	0·7787
	$Z_1/L = 0{\cdot}35$, $\alpha_1/D = 0{\cdot}45$				
0·1	0·9372	0·9521	0·9486	0·9523	0·9472
0·2	0·8966	0·9482	0·9935	0·9469	0·9308
0·3	0·8276	0·9405	0·9034	0·9376	0·8966
0·4	0·7451	0·9286	0·8575	0·9260	0·8429
0·5	0·6689	0·9124	0·7993	0·9139	0·7769

The first and second eigenfrequencies corresponding to the various crack conditions of both cracks are shown in Figures 4 and 5, respectively. The crack at the mid span has resulted in lower eigenfrequencies due to the reasons as explained earlier. But in Figure 5 the eigenfrequencies of the second mode for which the nodal point of the mode shape at the midpoint of the span gives one more piece of information about crack position: i.e., if the crack is located on a nodal point of a certain mode, the corresponding frequencies would be the same for all sizes of crack and the same in turn as those for no crack. The nodal point of a mode shape can be taken as "point of inflection" at which the bending moment vanishes [26].

A stability analysis is also carried out on the same rotor supported on rigid bearings as used in the eigenvalue analysis. The results are shown in Table 5. Since the system stability depends on internal damping, the viscous damping coefficient, $\eta_v = 0{\cdot}0002$ s and hysteretic damping, $\eta_H = 0{\cdot}00002$ are also included for the analysis.

Figure 6 shows the variation of normalized (with uncracked rotor) threshold speeds with crack parameters for the case of a mid span second crack and first crack at $Z_1/L = 0{\cdot}35$. Stability results are also obtained for the same rotor on

TABLE 4

Variation of normalized eigenfrequencies with cracks far off, $L/D = 8$, $Z_1/L = 0{\cdot}1$, $Z_2/L = 0{\cdot}85$

	α_1/D			
α_2/D	0·10	0·25	0·35	0·45
	I MODE			
0·1	0·9967	0·9887	0·9762	0·9519
0·2	0·9925	0·9846	0·9722	0·9485
0·3	0·9834	0·9757	0·9637	0·9408
0·4	0·9659	0·9588	0·9476	0·9259
0·5	0·9314	0·9254	0·9155	0·8963
	II MODE			
0·1	0·9892	0·9622	0·9219	0·8535
0·2	0·9747	0·9488	0·9102	0·8443
0·3	0·9444	0·9208	0·8854	0·8243
0·4	0·8909	0·8711	0·8407	0·7873
0·5	0·8034	0·7888	0·7655	0·7230
	III MODE			
0·1	0·9822	0·9382	0·8828	0·8144
0·2	0·9577	0·9162	0·8636	0·7979
0·3	0·9117	0·8744	0·8263	0·7648
0·4	0·8471	0·8148	0·7717	0·7145
0·5	0·7766	0·7485	0·7091	0·6544

flexible isotropic bearings of stiffness and damping values of 4×10^7 N/m and 10^3 Ns/m respectively (see Table 6).

The following observations can be made from the parametric study.

TABLE 5

Variation of normalized threshold speed with crack parameters for a rotor on rigid supports, $L/D = 8$

	Z_2/L				
α_2/D	0·15	0·3	0·5	0·7	0·85
	$Z_1/L = 0.35$, $\alpha_1/D = 0.1$				
0·1	0·9618	0·9605	0·9575	0·9587	0·9661
0·2	0·9474	0·9393	0·9280	0·9505	0·9587
0·3	0·9213	0·9193	0·9068	0·9375	0·9525
	$Z_1/L = 0{\cdot}35$, $\alpha_1/D = 0{\cdot}2$				
0·1	0·9312	0·9274	0·9262	0·9243	0·9274
0·2	0·9150	0·9113	0·9019	0·9183	0·9248
0·3	0·8954	0·8931	0·8869	0·9081	0·9193
	$Z_1/L = 0{\cdot}35$, $\alpha_1/D = 0{\cdot}25$				
0·1	0·9050	0·9032	0·9062	0·8950	0·9062
0·2	0·8950	0·8931	0·8856	0·8838	0·9019
0·3	0·8819	0·8769	0·8676	0·8738	0·8981

TABLE 6

Variation of normalized threshold speed with crack parameters for a rotor on flexible supports, $L/D = 8$

	Z_2/L				
α_2/D	0·15	0·3	0·5	0·7	0·85
	$Z_1/L = 0.35$, $\alpha_1/D = 0.1$				
0·1	0·9679	0·9671	0·9489	0·9706	0·9717
0·2	0·9499	0·9496	0·9315	0·9669	0·9669
0·3	0·9352	0·9351	0·9278	0·9597	0·9597
	$Z_1/L = 0{\cdot}35$, $\alpha_1/D = 0{\cdot}2$				
0·1	0·9415	0·9411	0·9296	0·9333	0·9442
0·2	0·9342	0·9324	0·9196	0·9260	0·9405
0·3	0·9233	0·9217	0·9179	0·9206	0·9388
	$Z_1/L = 0{\cdot}35$, $\alpha_1/D = 0{\cdot}25$				
0·1	0·9296	0·9296	0·9188	0·9224	0·9315
0·2	0·9251	0·9242	0·9124	0·9188	0·9297
0·3	0·9205	0·9198	0·9080	0·9224	0·9277

1. Any reduction in the eigenfrequency of a mode is largest if the cracks are near to each other and closer to the antinodal point of that mode shape.

2. When the distance between the cracks increases, the reduction in rotor eigenfrequencies are not significant even with deep cracks ($\bar{\alpha}_1 = \bar{\alpha}_2 = 0{\cdot}45$). But it is very significant for the third mode due to the reasons as stated in (1), the cracks are closer to the antinodal points.

3. Also it can be noticed that in the case of two cracks of different depths, the larger crack has the more significant effect on the eigenfrequency (Figure 2a).

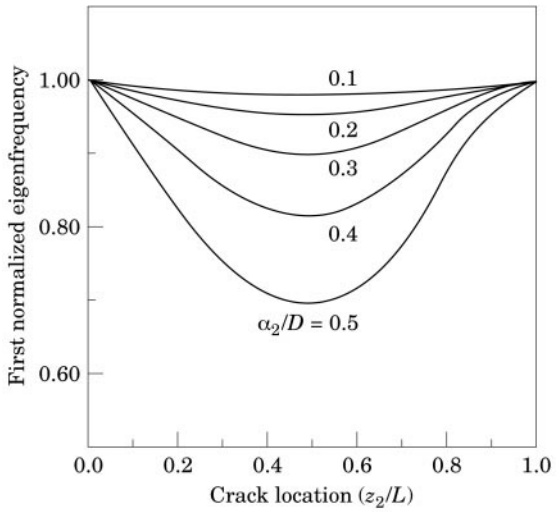

Figure 4. Variation of first eigenfrequency with depth and location of second crack, $Z_1/L = 0{\cdot}35$, $\alpha_1/D = 0{\cdot}1$.

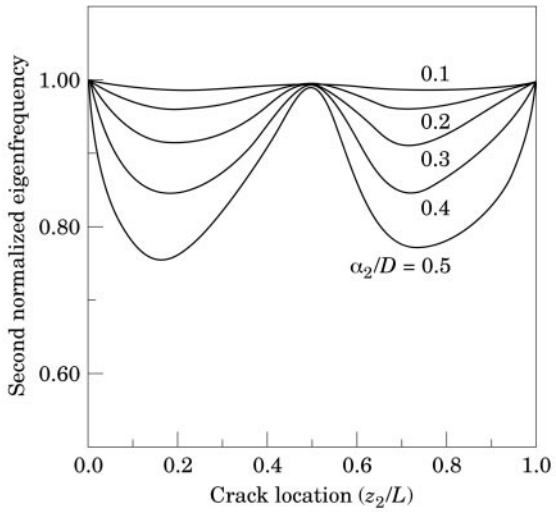

Figure 5. Variation of second eigenfrequency with depth and location of second crack, $Z_1/L = 0{\cdot}35$, $\alpha_1/D = 0{\cdot}1$.

4. The changes in eigenfrequencies due to cracks are appreciable in the cases of shafts with low slenderness ratio, L/D.

5. The effect of crack on the stability threshold is very significant for the case of a crack at the mid span. Even though the cracks are closer when $Z_1/L = 0{\cdot}35$ and $Z_2/L = 0{\cdot}3$ the effect on the stability limit is not significant (Table 5) as compared to that with mid span second crack. This is similar to the point 1.

6. Compared to the reduction in the eigenfrequencies with crack depth, the effect of rise in crack depth on the threshold speed limits is significant for the rotor considered here (see Figure 7). Also, it is noticed from Figure 7 that at certain speeds the eigenfrequency has reduced so much it becomes threshold speed. This reduction in threshold speed limits is reduced if the bearing supports are made flexible. However, the internal damping plays a significant role on the system stability of rotors. Hence, the effect of cracks together with different

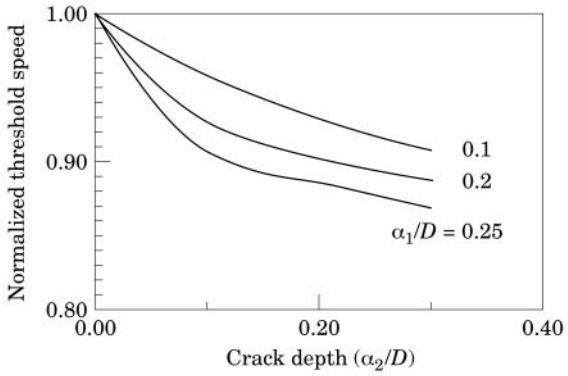

Figure 6. Variation of threshold speed with depths of cracks, $Z_1/L = 0{\cdot}35$, $Z_2/L = 0{\cdot}5$.

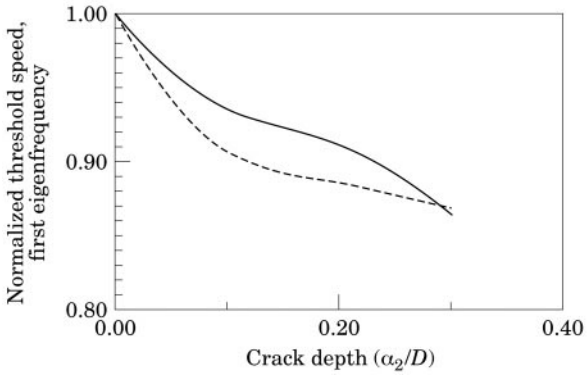

Figure 7. Comparison of normalized threshold speed with first eigenfrequency, $Z_1/L = 0{\cdot}35$, $Z_2/L = 0{\cdot}5$, $\alpha_1/D = 0{\cdot}25$: - - - -, threshold speed; ————, eigenfrequency.

internal damping values need to be analysed, before any definite conclusion can be made on the stability.

7. The increase in crack depth have a very significant effect on threshold stability speeds even for small crack depths, which is evident from Figure 7 and Tables 5 and 6.

Some observations are similar to those reported in [5] where only fundamental eigenfrequencies have been considered. The study has been carried out for two aligned cracks along the axis. However, this can be extended for two cracks in two different directions.

6. CONCLUSIONS

Finite element (FEM) modelling of a rotor-bearing system has been considered for the study of vibration characteristics of a rotor with two transverse open cracks.

The changes in eigenfrequencies due to cracks are appreciable in cases of shafts with low slenderness ratio, L/D.

It has been noticed that in the case of two cracks of different depths, the larger crack has the more significant effect on the eigenfrequency.

Compared to the reduction in eigenfrequencies with crack depth, the effect of cracks on threshold speed limits is significant. Also, the effect of a small crack on the stability speed is very much evident from the results.

ACKNOWLEDGMENTS

The author would like to acknowledge the assistance provided by Mr. J. K. Dey, graduate student in obtaining some numerical results.

REFERENCES

1. A. D. Dimarogonas and S. A. Paipetis 1983 *Analytical Methods in Rotor Dynamics*, London: Applied Science; 144–193.

2. J. WAUER 1990 *Applied Mechanics Reviews* **43**, 13–17. Dynamics of cracked rotors: literature survey.
3. R. GASCH 1993 *Journal of Sound and Vibration* **160**, 313–332. A survey of the dynamic behaviour of a simple rotating shaft with a transverse crack.
4. A. D. DIMAROGONAS 1996 *Engineering Fracture Mechanics* **55**, 831–857. Vibration of cracked structures: a state of the art review.
5. W. M. OSTACHOWICZ and M. KRAWEZUK 1991 *Journal of Sound and Vibration* **150**, 191–201. Analysis of effect of cracks on the natural frequencies of a cantilever beam.
6. M. H. SHEN and C. PIERRE 1990 *Journal of Sound and Vibration* **138**, 115–134. Natural modes of Bernoulli–Euler beams with symmetric cracks.
7. C. SURACE, R. RUOTOLO and C. MARES 1995 *Proceedings of ELFIN*3, *Costantza*, 210–219. Diagnosis of multiple damage in elastic structures.
8. R. RUOTOLO, C. SURACE and C. MARES 1996 *Proceedings of the* 14*th International Modal Analysis Conference*, 1560–1564. Theoretical and experimental study of the dynamic behaviour of a double-cracked beam.
9. R. RUOTOLO and C. SURACE 1997 *Journal of Sound and Vibration* **206**, 567–588. Damage assessment of multiple cracked beams: numerical results and experimental validation.
10. M. H. SHEN and J. E. TAYLOR 1991 *Journal of Sound and Vibration* **150**, 457–484. An identification problem for vibrating cracked beams.
11. R. RUOTOLO and C. SURACE 1996 *Proceedings ISMA*21, *Leuven, Belgium*, 1005–1016. Damage assessment for a beam with multiple cracks.
12. C. A. PAPADOPOULOS and A. D. DIMAROGONAS 1987 *Journal of Sound and Vibration* **117**, 81–93. Coupled longitudinal and bending vibrations of a rotating shaft with an open crack.
13. C. A. PAPADOPOULOS and A. D. DIMAROGONAS 1988 *Transactions of ASME, Journal of Vibration, Acoustics, Stress and Reliability in Design* **110**, 356–359. Stability of cracked rotors in the coupled vibration mode.
14. S. C. HUANG, Y. M. HUANG and S. M. SHIAH 1993 *Journal of Sound Vibration* **162**, 387–401. Vibration and stability of a rotating shaft containing a transverse crack.
15. C. H. CHUE, M. L. WU and C. H. CHANG 1993 *Engineering Fracture Mechanics* **45**, 479–486. Shearing effects on a shaft with circular surface crack under rotary bending.
16. Y. ISHIDA, T. YAMAMOTO and K. HIROKAWA 1994 *Proceedings of the Fourth International Conference Rotor Dynamics*, Chicago, IL, Sept 7–9, 47–52, Vibrations of a rotating shaft containing a transverse crack [Major critical speed of a horizontal shaft].
17. M. KRAWEZUK and W. M. OSTACHOWICZ 1992 *Archives of Applied Mechanics* **62**, 463–473. Parametric vibrations of beam with crack.
18. A. S. SEKHAR and B. S. PRABHU 1995 *Machine Vibration* **3**, 225–232. Condition monitoring of cracked rotors—a comparative study of fluid film bearing supports.
19. P. C. MULLER, J. BAJKOWSKI and D. SOFFKER 1994 *Nonlinear Dynamics* **5**, 233–254. Chaotic motions and fault detection in a cracked rotor.
20. H. D. NELSON and J. M. MCVAUGH 1976 *ASME Journal of Engineering for Industry* **98**, 593–600. The dynamics of rotor–bearing systems using finite elements.
21. H. N. OZGUVEN and Z. L. OZKAN 1984 *Transactions of ASME, Journal of Vibration, Acoustics, Stress and Reliability in Design* **106**, 72–79. Whirl speeds and unbalance response of multi bearing rotor using finite elements.
22. A. S. SEKHAR and B. S. PRABHU 1992 *Journal of Sound and Vibration* **157**, 375–381. Crack detection and vibration characteristics of cracked shafts.
23. G.-L. QIAN, S. N. GU and J.-S. JIANG 1990 *Journal of Sound and Vibration* **138**, 233–243. The dynamic behaviour and crack detection of a beam with a crack.

24. E. S. Zorzi and H. D. Nelson 1977 *Transactions of ASME, Journal of Engineering for Power* **99**, 71–76. Finite element simulation of rotor–bearing systems with internal damping.
25. H. D. Nelson 1980 *Transactions of ASME, Journal of Mechanical Design* **102**, 793–803, A finite rotating shaft element using Timoshenko beam theory.
26. T. C. Tsai and Y. Z. Wang 1996 *Journal of Sound and Vibration* **192**, 607–620. Vibration analysis and diagnosis of a cracked shaft.